

International Journal of Modern Physics E
 © World Scientific Publishing Company

RELATIVISTIC DESCRIPTION OF EXOTIC COLLECTIVE EXCITATION PHENOMENA IN ATOMIC NUCLEI

N. Paar

*Institut für Kernphysik, Technische Universität Darmstadt,
 Schlossgartenstrasse 9, D-64289 Darmstadt, Germany
 nils.paar@physik.tu-darmstadt.de*

T. Nikšić, D. Vretenar

Physics Department, Faculty of Science, University of Zagreb, Croatia

P. Ring

*Physik-Department der Technischen Universität München,
 D-85748 Garching, Germany*

Received (received date)

Revised (revised date)

The low-lying dipole and quadrupole states in neutron rich nuclei, are studied within the fully self-consistent relativistic quasiparticle random-phase approximation (RQRPA), formulated in the canonical basis of the Relativistic Hartree-Bogoliubov model (RHB), which is extended to include the density dependent interactions. In heavier nuclei, the low-lying E1 excited state is identified as a pygmy dipole resonance (PDR), i.e. as a collective mode of excess neutrons oscillating against a proton-neutron core. Isotopic dependence of the PDR is characterized by a crossing between the PDR and one-neutron separation energies. Already at moderate proton-neutron asymmetry the PDR peak is calculated above the neutron emission threshold, indicating important implications for the observation of the PDR in (γ, γ') scattering, and on the theoretical predictions of the radiative neutron capture rates in neutron-rich nuclei. In addition, a novel method is suggested for determining the neutron skin of nuclei, based on measurement of excitation energies of the Gamow-Teller resonance relative to the isobaric analog state.

1. Introduction

The multipole excitation phenomena in exotic nuclei, in particular the properties of the low-energy excited states have raised significant interest in many recent theoretical and experimental studies. As one moves away from the valley of β -stability towards the neutron rich side, modification of the effective nuclear potential leads to the formation of nuclei with diffuse neutron densities, the occurrence of the neutron skin, halo structures, and new modes of excitations. The weak binding of outermost neutrons might give rise to the existence of pygmy dipole resonance (PDR), when loosely bound neutrons coherently oscillate against the proton-neutron core^{1,2}.

2 *N. Paar, T. Nikšić, D. Vretenar, and P. Ring*

The onset of low-energy E1 strength has been observed in electromagnetic excitations in heavy-ion collisions in oxygen isotopes ³, and via (γ, γ') scattering in lead isotopes ^{4,5} and N=82 ^{6,7} isotone chain. Although the low-lying excitations have been observed below or near the particle threshold, their structure and collectivity still remain under discussion ^{8,9,10,11}. Recent study within the quasiparticle phonon model have shown that the low-lying excitations corresponding to the pygmy dipole resonance are closely related to the size of the neutron skin ¹². However, it has also been suggested that the low-lying E1 strength could be of different origin ⁶. In addition to the two-phonon $2^+ \otimes 3^-$ state, and the pygmy state, in this energy region one could also expect some compressional low-lying isoscalar dipole strength, maybe mixed with toroidal states ¹³, as well as the E1 strength generated by the breaking of the isospin symmetry due to a clustering mechanism ¹⁴. The low-lying excited states in weakly bound nuclei are well described by the quasiparticle random phase approximation (QRPA) based on the HFB ground state. In a recent study, the relativistic QRPA has been formulated in the canonical basis of the relativistic Hartree-Bogoliubov model ¹⁰, and it has also been extended for the studies of charge exchange excitations ¹⁵. For understanding of the r-process, the properties of Gamow-Teller ($J^\pi = 1^+$) resonances (GTR) in nuclei towards the neutron drip-line are of a particular importance, since the half-lives of β -decays along the r-process path are generally dominated by the low-energy tails of GTR. The excitation energies of the spin-flip and isospin-flip modes can also provide information on the neutron skin of atomic nuclei ¹⁶.

2. Self-consistent relativistic quasiparticle RPA in the relativistic Hartree-Bogoliubov model

In relativistic mean field models, the nucleus is described as a system of Dirac nucleons that interact in a relativistic covariant manner by exchange of effective mesons. A quantitative theoretical description of complex nuclear systems necessitates a density dependent interaction, which is introduced via nonlinear σ self-interaction, or by explicitly including phenomenological density dependence of σ , ω , and ρ meson-nucleon vertex functions, adjusted to the properties of nuclear matter and finite nuclei ¹⁷. The present investigation is based on the density dependent effective interaction DD-ME1 ¹⁷. In comparison to the interactions with non-linear σ -meson self-interaction ^{18,19}, the properties of asymmetric nuclear matter are much better described by DD-ME1 interaction, and its improved isovector properties result in better description of charge radii and neutron skin, what is essential for the studies of exotic nuclei. Description of the ground state in unstable open shell nuclei, characterized by the closeness of the Fermi surface to the particle continuum, necessitates a unified description of mean-field and pairing correlations, as for example in the framework of the Relativistic Hartree-Bogoliubov (RHB) theory. The pairing correlations in RHB model are described by the finite range Gogny interaction D1S ²⁰. Excitations are studied within the relativistic quasiparticle random-phase

Table 1. Integrated energy weighted dipole strength in oxygen isotopes up to 15 MeV in excitation energy, given in units of the TRK sum rule[%].

Oxygen isotope A =	18	20	22	24
RHB+RQRPA(DD-ME1)	11.7	11.9	15.2	20.9
continuum QRPA ²²	7	11	16	21
Shell model ²³	6.4	10.9	10.0	8.6
QRPA + phonon coupling ²⁴	7.0	9.0	7.5	
Experiment (GSI) ³	8	12	7	

approximation (RQRPA) in the configurational space, which is derived from the time-dependent RHB model in the limit of small amplitude vibrations ^{10,21}. The RQRPA equations are formulated in the canonical single-nucleon basis of RHB model which involves discretization of both the occupied states and the continuum. In order to describe transitions to low-lying excited states in weakly bound nuclei, the two-quasiparticle configuration space must include states with both nucleons in the discrete bound levels, states with one nucleon in the bound level and one nucleon in the continuum, and also states with both nucleons in the continuum. In addition, a consistent treatment of the Dirac sea of negative energy states is essential for successful application of RQRPA model. The present RHB+RQRPA model is fully self-consistent, i.e. the same effective interactions in ph and pp channels, are used both in the RHB calculation for the ground state and in RQRPA residual interaction, in order to recover the sum-rules and to decouple the spurious states.

3. Low-lying multipole excitations in exotic nuclei

As one moves towards nuclei away from the valley of β stability, in addition to giant resonances, additional exotic excitations may appear in the low-energy region. In the present study, the fully self-consistent RHB+RQRPA model, based on interactions with density dependent couplings, is used to investigate the properties of low-lying multipole excitations as approaching towards exotic nuclei. As the neutron number increases along the isotope chain, the isovector dipole strength distribution is characterized by its spreading into the low-energy region, and by the mixing of isoscalar and isovector modes ¹⁰.

In Table 1 RHB+RQRPA low-lying E1 strength ($E < 15 MeV$) is compared with non-relativistic models: continuum linear response theory based on HFB ground state ²², shell model calculations ²³, and QRPA plus phonon coupling model (with the neutron pairing gap $\Delta_n = 12/\sqrt{A} MeV$) ²⁴, in comparison with the systematic experimental data from electromagnetic excitations in the heavy-ion collisions ³. For isotopes heavier than ²⁰O the agreement of RHB+RQRPA results with experiment is less satisfactory; partly it is due to the fact that in the RHB model the drip-line for $Z=8$ is approached at ²⁸O, instead ²⁴O. The low-energy dipole strength in light nuclei is composed from the non-resonant single particle excitations of loosely bound neutrons, and therefore it does not correspond to the collective PDR mode ⁹.

4 *N. Paar, T. Nikšić, D. Vretenar, and P. Ring*

However, the underlying structure of the low-lying dipole strength changes with the mass number. In neutron-rich medium-heavy and heavy nuclei, a collective PDR state appears in the low-energy region due to vibration of neutrons from the outer orbitals which give rise of the neutron skin⁹. In the present study, we extend investigation from Ref.⁹ by employing RHB+RQRPA model with density-dependent interaction DD-ME1, which properly describes the size of neutron skin. In Fig. 1 we

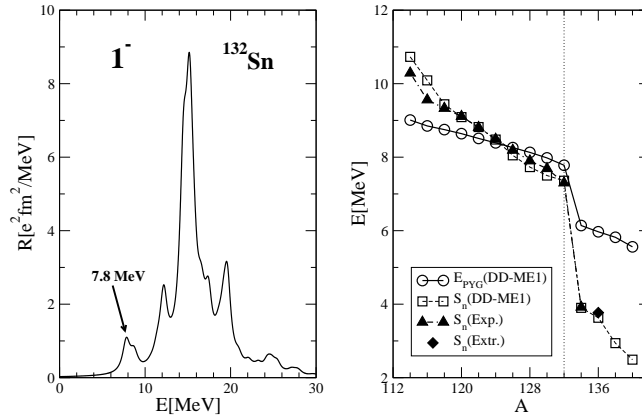


Fig. 1. RHB+RQRPA strength distribution of isovector dipole excitations in ^{132}Sn , calculated with DD-ME1 effective interaction (left panel). The PDR excitation energies and one-neutron separation energies are displayed as a functions of the mass number for Sn isotopes, and compared with the experimental and extrapolated values²⁵ (right panel).

show the isovector dipole strength distribution in ^{132}Sn . In addition to the characteristic peak of the isovector giant dipole resonance (IVGDR) at 15.2 MeV, among several dipole states in the low-energy region between 7 MeV and 10 MeV that are characterized by single particle transitions, at 7.8 MeV a single pronounced peak is found with a more distributed structure of the RQRPA amplitude, exhausting 1.6% of the energy weighted sum rule (EWSR), where $\text{EWSR}=(1+\kappa)\text{TRK}$. Here TRK corresponds to the classical Thomas-Reiche-Kuhn sum rule²³, and the enhancement factor from calculation equals $\kappa=0.35$. The peak at 7.8 MeV is composed mainly of 11 neutron ph transitions from loosely bound orbits, each contributing more than 0.1% to the total RRPAA amplitude $\sum_{\bar{p}h} |X_{\bar{p}h}^v|^2 - |Y_{\bar{p}h}^v|^2 = 1$, where X^v and Y^v are RRPAA eigenvectors. As we have shown in Refs.^{9,10} by analyzing the corresponding transition densities, the dynamics of this low-energy mode is very different from that of the IVGDR: the proton and neutron transition densities are in phase in the nuclear interior, there is almost no contribution from the protons in the surface region, the isoscalar transition density dominates over the isovector one in the interior, and the large neutron component in the surface region contributes to the formation of a node in the isoscalar transition density. The low-lying pygmy

state does not belong to statistical E1 excitations sitting on the tail of the GDR, but represents a fundamental structure effect: the neutron skin oscillates against the core. In the right panel of Fig. 1, RHB+RQRPA peak energies of PDR are plotted as function of the mass number for Sn isotopes, in comparison with the calculated one-neutron separation energies and the corresponding experimental data and the extrapolated value ²⁵. One can observe that PDR excitation energy monotonously decreases with the mass number, but a small kink appears at $N = 82$ shell closure. The calculated one-neutron separation energies of the Sn nuclei reproduce experimental data in detail. However, the separation energies decrease much faster than the calculated PDR excitation energies. At $N = 82$, in particular, the separation energies display a sharp decrease, whereas the shell closure produces only a weak effect on the PDR excitation energies. The important result here is that for $A < 124$ the PDR excitation energies are lower than the corresponding one-neutron separation energies, whereas for $A \geq 124$ the pygmy resonance is located above the neutron emission threshold. This means, of course, that in the latter case the observation of the PDR in (γ, γ') experiments will be strongly hindered. The relative position of the PDR with respect to the neutron emission threshold will also have an effect on the calculated cross sections for radiative neutron capture in neutron-rich Sn nuclei ^{26,27}.

Another example how the exotic nuclear structure of loosely bound nucleons may affect the properties of excitation phenomena, can be observed in quadrupole excitations. The low-lying 2^+ states in the neutron rich oxygen isotopes have been already studied in the self-consistent Skyrme Hartree-Fock-BCS + QRPA, demonstrating that in exotic nuclei the neutron to proton transition amplitudes for low-lying states differ noticeably from the simple N/Z estimate ²⁸. The evolution of the low-lying 2^+ strength strongly depends on the size of neutron excess ²⁹. The position of the low-lying 2^+ state is highly sensitive to the pairing correlations, and it is essential to include the pairing interaction in a fully self-consistent way both in the ground state and in the residual RPA interaction ^{22,10}. In Fig. 2 we plot the isovector and isoscalar quadrupole strength distribution in ²²O. The strong peak at $E \approx 23$ MeV in the isoscalar strength function corresponds to the isoscalar giant quadrupole resonance. The low-lying state is located at 3.0 MeV, in fair agreement with observed value at 3.2 MeV ³³. The isovector response, on the other hand, is strongly fragmented, and distributed over the large region of excitation energies $E \simeq 17 - 38$ MeV. In the right panel on Fig. 2 we compare the RHB+RQRPA energies and transition probabilities $B(E2)$ of the low-lying 2^+ state in oxygen isotopes, with results of previous studies. The calculated excitation energies of the first 2^+ state in general slightly overestimate the measured excitation energies, except in ²²O. The RHB+RQRPA results for the low-lying 2^+ excitation energies are qualitatively in agreement with non-relativistic QRPA calculations of the quadrupole response in neutron rich oxygen isotopes ^{28,30,29}. The $B(E2)$ values are obtained above the other theoretical predictions, and only in ²⁰O the experimental data is reproduced.

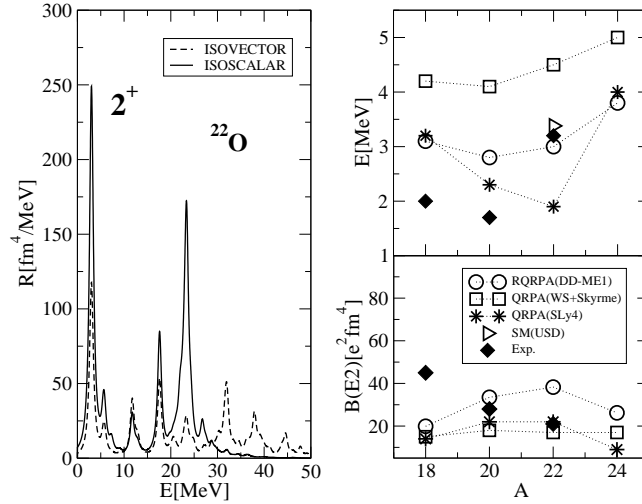
6 *N. Paar, T. Nikšić, D. Vretenar, and P. Ring*


Fig. 2. RHB+RQRPA (DD-ME1) strength distribution of isovector and isoscalar quadrupole response in ^{22}O (left panel). The calculated energies and $B(E2)$ values of low-lying 2^+ states in oxygen isotopes are compared with nonrelativistic QRPA^{29,30}, shell model calculations³¹ and experimental data^{32,33} (right panel).

4. Spin-isospin resonances and the neutron skin in nuclei

The use of giant resonances is one among various experimental methods that have been employed in the past to measure the size of the neutron skin³⁴. In the following, a new method is suggested for determining the difference between the radii of the neutron and proton density distributions along an isotopic chain, based on measurement of the excitation energies of the Gamow-Teller resonances (GTR) relative to the isobaric analog states (IAR)¹⁶. For the purpose of the present study, the RHB+RQRPA model has been extended to treat the charge-exchange excitations - PN-RQRPA¹⁵. In addition to ρ -meson exchange in the residual interaction, the pion with pseudo-vector type of meson-nucleon coupling is also included to investigate unnatural parity excitations. Because of the derivative type of the pion-nucleon coupling, it is also necessary to include a zero-range Landau-Migdal term that accounts for the contact part of the nucleon-nucleon interaction. It comes with a parameter $g' = 0.55$, adjusted to reproduce experimental data on the GTR excitation energies. In the present analysis we also use the Gogny interaction in the $T = 1$ pp -channel of the PN-RQRPA. For the $T = 0$ proton-neutron pairing interaction in open shell nuclei we employ a similar interaction: a short-range repulsive Gaussian combined with a weaker longer-range attractive Gaussian¹⁵. IAR strength distributions, i.e. the $J^+ = 0^+$ states, are generated by the Fermi transition operator $T_{\beta\pm}^F = \sum_{i=1}^A \tau_{\pm}$. On the other hand, GTR represents a coherent superposition of high-lying $J^{\pi} = 1^+$ proton-particle - neutron-hole configurations of maximum

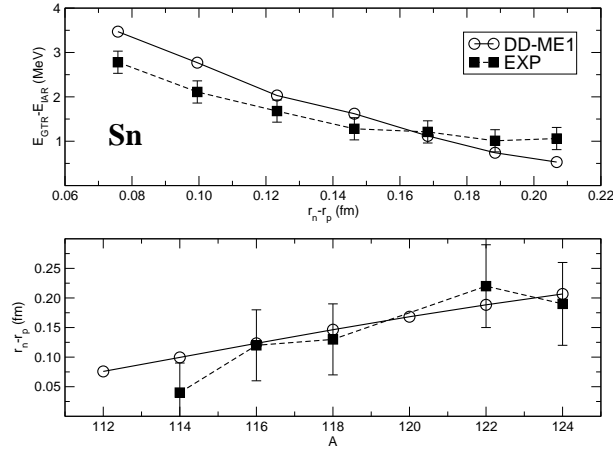


Fig. 3. The proton-neutron RQRPA and experimental ³⁵ differences between the excitation energies of the GTR and IAR, as a function of the calculated differences between the rms radii of the neutron and proton density distributions of even-even Sn isotopes (upper panel). In the lower panel the calculated differences $r_n - r_p$ are compared with experimental data ³⁴.

collectivity associated with charge-exchange excitations of neutrons from orbitals with $j = l + 1/2$ into proton orbitals with $j = l - 1/2$. The GT operator reads, $T_{\beta^\pm}^{GT} = \sum_{i=1}^A \Sigma \tau_{\pm}$. In Fig. 3 we display the calculated differences between the centroids of the direct spin-flip GT strength and the respective isobaric analog resonances for the sequence of even-even Sn target nuclei. For $A = 112 - 124$ the results of RHB plus proton-neutron RQRPA calculation (DD-ME1 density-dependent effective interaction, Gogny $T = 1$ pairing, $T = 0$ pairing interaction ¹⁵ with $V_0 = 250$ MeV, the Landau-Migdal parameter $g' = 0.55$), are compared with experimental data ³⁵. As it has been emphasized in Ref. ¹⁶, the energy difference between the GTR and the IAS reflects the magnitude of the effective spin-orbit potential. One can observe a uniform dependence of the energy spacings between the GTR and IAS on the size of the neutron-skin. In principle, therefore, the value of $r_n - r_p$ can be determined from the theoretical curve for a given value of $E_{\text{GT}} - E_{\text{IAS}}$. Of course, this necessitates implementation of a model which reproduces the experimental values of the $r_n - r_p$, as it is displayed for RHB by using DD-ME1 effective interaction for Sn isotopes in the lower panel of Fig. 3.

5. Conclusions

In summary, the RHB plus relativistic QRPA which is extended to include the interactions with density dependent meson-nucleon coupling constants (DD-ME1), represents an advanced microscopic fully self-consistent model to investigate the properties of low-lying excitations in neutron-rich nuclei. It is demonstrated that the one-neutron separation energies in Sn isotopes decrease much faster with the

8 *N. Paar, T. Nikšić, D. Vretenar, and P. Ring*

mass number than PDR excitation energies, resulting with a characteristic crossing already at moderate neutron-proton asymmetry. Finally, it is also shown that the energy spacings between the GTR and IAS provide direct information on the evolution of neutron skin-thickness along the Sn isotopic chain.

Acknowledgments

This work has been supported in part by the Bundesministerium für Bildung und Forschung under project 06 MT 193, and by the Gesellschaft für Schwerionenforschung (GSI) Darmstadt. N.P. acknowledges support from the Deutsche Forschungsgemeinschaft (DFG) under contract SFB 634.

References

1. Y. Suzuki et al., *Prog. Theor. Phys.* **83**, 180 (1990).
2. J. Chambers et al., *Phys. Rev.* **C 50**, R2671 (1994).
3. A. Leistenschneider et al., *Phys. Rev. Lett.* **86**, 5442 (2001).
4. N. Ryezayeva et al., *Phys. Rev. Lett.* **89**, 272502 (2002).
5. J. Enders et al., *Nucl. Phys.* **A 724**, 243 (2003).
6. A. Zilges et al., *Phys. Lett.* **B 542**, 43 (2002).
7. A. Zilges, *Nucl. Phys.* **A 731**, 249 (2004).
8. J. P. Adams, B. Castel, and H. Sagawa, *Phys. Rev.* **C 53**, 1016 (1996).
9. D. Vretenar, N. Paar, P. Ring, and G. A. Lalazissis *Nucl. Phys.* **A 692**, 496 (2001).
10. N. Paar, T. Nikšić, D. Vretenar, and P. Ring, *Phys. Rev.* **C 67**, 034312 (2003).
11. D. Sarchi, P. F. Bortignon, and G. Colo, *nucl-th/0406076* (2004).
12. N. Tsoneva, H. Lenske, and Ch. Stoyanov, *Phys. Lett.* **B 586**, 213 (2004).
13. D. Vretenar, N. Paar, P. Ring, and T. Nikšić, *Phys. Rev.* **C 65**, 021301 (2002).
14. F. Iachello, *Phys. Rev. Lett.* **53**, 1427 (1984).
15. N. Paar, T. Nikšić, D. Vretenar, and P. Ring, *Phys. Rev.* **C 69**, 054303 (2004).
16. D. Vretenar, N. Paar, T. Nikšić, and P. Ring, *Phys. Rev. Lett.* **91**, 262502 (2003).
17. T. Nikšić et al., *Phys. Rev.* **C 66**, 024306 (2002).
18. P.G. Reinhard et al., *Z. Phys.* **A323**, 13 (1986).
19. G.A. Lalazissis, J. König, and P. Ring, *Phys. Rev.* **C 55**, 540 (2003).
20. J.F. Berger and M. Girod and D. Gogny, *Nucl. Phys.* **A 428**, 32 (1984).
21. T. Nikšić, D. Vretenar, and P. Ring, *Phys. Rev.* **C 66**, 064302 (2002).
22. M. Matsuo, *Nucl. Phys.* **A 696**, 371 (2001).
23. H. Sagawa and T. Suzuki, *Nucl. Phys.* **A 687**, 111c (2001).
24. G. Coló and P. F. Bortignon, *Nucl. Phys.* **A 696**, 427 (2001).
25. G. Audi and A. H. Wapstra, *Nucl. Phys.* **A 595**, 409 (1995).
26. S. Goriely, *Phys. Lett.* **B 436**, 10 (1998).
27. S. Goriely and E. Khan, *Nucl. Phys.* **A 706**, 217 (2002).
28. E. Khan and N. Van Giai, *Phys. Lett.* **B 472**, 253 (2000).
29. M. Matsuo, *Prog. Theor. Phys. Supp.* **146**, 110 (2002).
30. E. Khan et al., *Phys. Rev.* **C 66**, 024309 (2002).
31. P. G. Thirolf et al., *Phys. Lett.* **B 485**, 16 (2000).
32. S. Raman et. al., *Atomic Data and Nuclear Data Tables* **36**, 1 (1987).
33. M. Belleguic et al., *Nucl. Phys.* **A 682**, 136c (2001).
34. A. Krasznahorkay et al., *Phys. Rev. Lett.* **82**, 3216 (1999).
35. K. Pham et al., *Phys. Rev.* **C 51**, 526 (1995).